

# Representing Graphs and Hypergraphs by Touching Polygons in 3D<sup>\*</sup>

William Evans<sup>1</sup>, Paweł Rzażewski<sup>2</sup>[0000–0001–7696–3848], Noushin Saeedi<sup>1</sup>,  
Chan-Su Shin<sup>3</sup>[0000–0003–3073–6863], and Alexander Wolff<sup>4</sup>[0000–0001–5872–718X]

<sup>1</sup> University of British Columbia, Vancouver, Canada

<sup>2</sup> Warsaw University of Technology, Faculty of Mathematics and Information Science,  
Warszawa, Poland

<sup>3</sup> Hankuk University of Foreign Studies, Yongin, Republic of Korea

<sup>4</sup> Universität Würzburg, Würzburg, Germany

*Dedicated to Honza Kratochvíl on his 60th birthday.*

**Abstract.** Contact representations of graphs have a long history. Most research has focused on problems in 2d, but 3d contact representations have also been investigated, mostly concerning fully-dimensional geometric objects such as spheres or cubes. In this paper we study contact representations with convex polygons in 3d. We show that every graph admits such a representation. Since our representations use super-polynomial coordinates, we also construct representations on grids of polynomial size for specific graph classes (bipartite, subcubic). For hypergraphs, we represent their duals, that is, each vertex is represented by a point and each edge by a polygon. We show that even regular and quite small hypergraphs do not admit such representations. On the other hand, the Steiner triple systems  $S(2, 3, 7)$  and  $S(2, 3, 9)$  can be represented.

## 1 Introduction

Representing graphs as the contact of geometric objects has been an area of active research for many years (see Hliněný and Kratochvíl’s survey [14] and Alam’s thesis [1]). Most of this work concerns representation in two dimensions, though there has been some interest in three-dimensional representation as well [2, 3, 5, 12, 23]. Representations in 3d typically use 3d geometric objects that touch properly i.e., their intersection is a positive area 2d face. In contrast, our main focus is on contact representation of graphs and hypergraphs using non-intersecting (open, “filled”) planar polygons in 3d. Two polygons are in *contact* if they share a corner vertex. Note that two triangles that share two corner vertices do not intersect and a triangle and rectangle that share two corners,

---

<sup>\*</sup> W.E. and N.S. were funded by an NSERC Discovery grant and in part by the Institute for Computing, Information and Cognitive Systems (ICICS) at UBC. P.Rz. was partially supported by the ERC grant CUTACOMBS (no. 714704). A.W. was funded by the German Research Foundation (DFG) under grant 406987503 (WO 758/10-1). C.-S.Sh. was supported by the National Research Foundation of Korea (NRF) grant funded by the Korea government (MSIT) (no. 2019R1F1A1058963).

even diagonally opposite ones, also do not intersect. However, no polygon contains a corner of another except at its own corner. A *contact representation of a graph in 3d* is a set of non-intersecting polygons in 3d that represent vertices. Two polygons share a corner point if and only if they represent adjacent vertices and each corner point corresponds to a distinct edge. We can see a contact representation of a graph  $G = (V, E)$  as a certain drawing of its *dual hypergraph*  $H_G = (E, \{E(v) \mid v \in V\})$  which has a vertex for every edge of  $G$ , and a hyperedge for every vertex  $v$  of  $G$ , namely the set  $E(v)$  of edges incident to  $v$ . We extend this idea to arbitrary hypergraphs: A *non-crossing drawing of a hypergraph in 3d* is a set of non-intersecting polygons in 3d that represent *edges*. Two polygons share a corner point if and only if they represent edges that contain the same vertex and each corner point corresponds to a distinct vertex. It is straightforward to observe that the set of contact representations of a graph  $G$  is the same as the set of non-crossing drawings of  $H_G$ .

Many people have studied ways to represent hypergraphs geometrically [4, 6, 15], perhaps starting with Zykov [27]. A natural motivation of this line of research was to find a nice way to represent combinatorial configurations [13] such as Steiner systems (for an example, see Fig. 7). The main focus in representing hypergraphs, however, was on drawings in the plane. By using polygons to represent hyperedges in 3d, we gain some additional flexibility though still not all hypergraphs can be realized. Our work is related to Carmensin’s work [8] on a Kuratowski-type characterization of 2d simplicial complexes (sets composed of points, line segments, and triangles) that have an embedding in 3-space. Our representations are sets of planar polygons (not just triangles) that arise from hypergraphs. Thus they are less expressive than Carmensin’s topological 2d simplicial complexes and are more restricted. In particular, if two hyperedges share three vertices, the hyperedges must be coplanar in our representation.

*Our contribution.* All of our representations in this paper use convex polygons while our proofs of non-representability hold even permitting non-convex polygons. We first show that recognizing segment graphs in 3d is  $\exists\mathbb{R}$ -complete.

We show that every graph on  $n$  vertices with minimum vertex-degree 3 has a contact representation by convex polygons in 3d, though the volume of the drawing using integer coordinates is at least exponential in  $n$ ; see Section 2.

For some graph classes, we give 3d drawing algorithms which require polynomial volume. Table 1 summarizes our results. When we specify the volume of the drawing, we take the product of the number of grid lines in each dimension (rather than the volume of a bounding box), so that a drawing in the xy-plane has non-zero volume. Some graphs, such as the squares of even cycles, have particularly nice representations using only unit squares; see Appendix B.2.

For hypergraphs our results are more preliminary. There are examples as simple as the hypergraph on six vertices with all triples of vertices as hyperedges that cannot be drawn using non-intersecting polygons; see Section 3. For certain very symmetric hypergraphs, we can show that such drawings do exist. These hypergraphs are part of a family called Steiner systems, though, as we show, not all members of this family have such representations.

**Table 1:** Required volume and running times of our algorithms for drawing  $n$ -vertex graphs of certain graph classes in 3d

Graph class	general	bipartite	1-plane cubic	2-edge-conn. cubic	subcubic
Grid volume	super-poly	$O(n^4)$	$O(n^2)$	$O(n^2)$	$O(n^3)$
Running time	$O(n^2)$	linear	linear	$O(n \log^2 n)$	$O(n \log^2 n)$
Reference	Theorem 2	Theorem 3	Theorem 4	Lemma 2	Theorem 5

## 2 Graphs

It is easy to draw graphs in 3d using points as vertices and non-crossing line segments as edges – any set of points in general position (no three colinear and no four coplanar) will support any set of edge segments without crossings. A more difficult problem is to represent a graph in 3d using polygons as vertices where two polygons intersect to indicate an edge (note that here we do not insist on a *contact representation*, i.e., polygons are allowed to intersect arbitrarily). Intersection graphs of convex polygons in 2d have been studied extensively [18]. Recognition is  $\exists\mathbb{R}$ -complete [21] (and thus in PSPACE since  $\exists\mathbb{R} \subseteq \text{PSPACE}$  [7]) even for segments (polygons with only two vertices).

Every complete graph trivially admits an intersection representation by line segments in 2d. Not every graph, however, can be represented in this way, see e.g., Kratochvíl and Matoušek [17]. Moreover, they show that recognizing intersection graphs of line segments in the plane, called *segment graphs*, is  $\exists\mathbb{R}$ -complete. It turns out that a similar hardness result holds for recognizing intersection graphs of straight-line segments in 3d (and actually in any dimension). The proof modifies the corresponding proof for 2d by Schaefer [21]. See also the excellent exposition of the proof by Matoušek [19]. For the proof, as well as the proofs of other theorems marked with ♠, see the appendix. In particular, the proof of Theorem 1 is in Appendix A.

**Theorem 1 (♠).** *Recognizing segment graphs in 3d is  $\exists\mathbb{R}$ -complete.*

We consider *contact representation* of graphs in 3d where no polygons are allowed to intersect except at their corners, and two polygons share a corner if and only if they represent adjacent vertices. We start by describing how to construct a contact representation for any graph using convex polygons, which requires at least exponential volume, and then describe constructions for graph families that use only polynomial volume.

### 2.1 General Graphs

**Lemma 1.** *For every positive integer  $n \geq 3$ , there exists an arrangement of  $n$  lines  $\ell_1, \ell_2, \dots, \ell_n$  with the following two properties:*

(A1) *line  $\ell_i$  intersects lines  $\ell_1, \ell_2, \dots, \ell_{i-1}, \ell_{i+1}, \dots, \ell_n$  in this order, and*

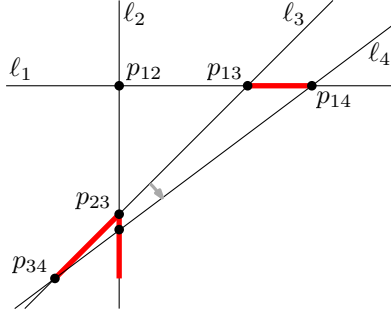


**Fig. 1:** Construction of  $\ell_4$  in the proof of Lemma 1.

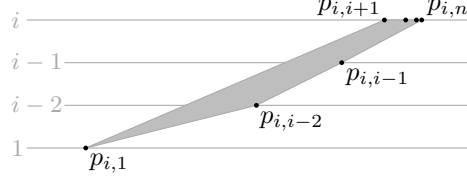


**Fig. 2:** The polygon  $P_i$  that represents vertex  $i$  of  $K_n$ .

(A2) *distances between the intersection points on line  $\ell_i$  decrease exponentially, i.e., for every  $i$  it holds that*

$$d_i(j+2, j+1) \leq d_i(j+1, j)/2 \quad \text{for } j \in \{1, \dots, i-3\} \quad (1)$$

$$d_i(i+1, i-1) \leq d_i(i-1, i-2)/2 \quad (2)$$

$$d_i(i+2, i+1) \leq d_i(i+1, i-1)/2 \quad (3)$$

$$d_i(j+2, j+1) \leq d_i(j+1, j)/2 \quad \text{for } j \in \{i+1, \dots, n-2\}, \quad (4)$$

where  $d_i(j, k)$  is the  $xy$ -plane distance between  $p_{i,j}$  and  $p_{i,k}$  and  $p_{i,j} = p_{j,i}$  is the intersection point of  $\ell_i$  and  $\ell_j$ .

*Proof.* We construct the grid incrementally. We start with the  $x$ -axis as  $\ell_1$ , the  $y$ -axis as  $\ell_2$ , and the line through  $(1, 0)$  and  $(0, -1)$  as  $\ell_3$ ; see Fig. 1. Now suppose that  $i > 3$ , we have constructed lines  $\ell_1, \ell_2, \dots, \ell_{i-1}$ , and we want to construct  $\ell_i$ . We fix  $p_{i-1,i}$  to satisfy  $d_{i-1}(i, i-2) = d_{i-1}(i-2, i-3)/2$  then rotate a copy of line  $\ell_{i-1}$  clockwise around  $p_{i-1,i}$  until it (as  $\ell_i$ ) satisfies another of the inequalities in (1) with equality. Note that during this rotation, all inequalities in (A2) are satisfied and we do not move any previously constructed lines, so the claim of the lemma follows.  $\square$

**Theorem 2.** *For every  $n \geq 3$ , the complete graph  $K_n$  admits a contact representation by non-degenerate convex polygons in  $3d$ , each with at most  $n-1$  vertices. Such a representation can be computed in  $O(n^2)$  time (assuming unit cost for arithmetic operations on coordinates).*

*Proof.* Take a grid according to Lemma 1. Set the  $z$ -coordinate of point  $p_{i,j}$  to  $\min\{i, j\}$  and represent vertex  $i$  by the polygon  $P_i$ , which we define to be the convex hull of  $\{p_{i,1}, p_{i,2}, \dots, p_{i,i-1}, p_{i,i+1}, \dots, p_{i,n}\}$ . Note that  $P_i$  is contained in the vertical plane that contains line  $\ell_i$ ; see Fig. 2. To avoid that  $P_1$  is degenerate, we reduce the  $z$ -coordinate of  $p_{1,2}$  slightly.

Note that, for  $i = 2, \dots, n-1$ , the counterclockwise order of the vertices around  $P_i$  is

$$p_{i,1}, p_{i,2}, \dots, p_{i,i-1}, p_{i,n}, p_{i,n-1}, \dots, p_{i,i+1}, p_{i,1}.$$

We show that all these points are on the boundary of  $P_i$  by ensuring that the angles formed by three consecutive points are bounded by  $\pi$ . Clearly the angles  $\angle p_{i,i+1}p_{i,1}p_{i,2}$  and  $\angle p_{i,i-1}p_{i,n}p_{i,n-1}$  are at most  $\pi$ . For  $j = 2, \dots, i-2$ , we have that  $\angle p_{i,j-1}p_{i,j}p_{i,j+1} < \pi$ , which is due to the fact that the z-coordinates increase in each step by 1, while the distances decrease (property (A2)). Note that  $\angle p_{i,i+1}, p_{i,i+2}, p_{i,i+3} = \dots = \angle p_{i,n-2}, p_{i,n-1}, p_{i,n} = \pi$ . Finally, we claim that  $\angle p_{i,i-2}, p_{i,i-1}, p_{i,n} < \pi$ . Clearly,  $z(p_{i,i-1}) - z(p_{i,i-2}) = 1 = z(p_{i,n}) - z(p_{i,i-1})$ . The claim follows by observing that, due to property (A2) and the geometric series formed by the distances,

$$d_i(i-1, n) = d_i(i-1, i+1) + \sum_{k=i+1}^{n-1} d_i(k, k+1) < 2d_i(i-1, i+1) \leq d_i(i-2, i-1).$$

It remains to show that, for  $1 \leq i < j \leq n$ , polygons  $P_i$  and  $P_j$  do not intersect other than in  $p_{i,j}$ . This is simply due to the fact that  $P_j$  is above  $P_i$  in  $p_{i,j}$ , and lines  $\ell_i$  and  $\ell_j$  only intersect in (the projection of) this point.  $\square$

**Corollary 1.** *Every graph with minimum vertex-degree 3 admits a contact representation by convex polygons in 3d.*

*Proof.* Let  $n$  be the number of vertices of the given graph  $G = (V, E)$ . We use the contact representation of  $K_n$  and modify it as follows. For every pair  $\{i, j\} \notin E$ , just remove the point  $p_{i,j}$  before defining the convex hulls.  $\square$

We can make the convex polygons of our construction strictly convex if we slightly change the z-coordinates. For example, decrease the z-coordinate of  $p_{i,j}$  by  $\delta/d_{\min\{i,j\}}(1, \max\{i, j\})$ , where  $\delta$  is such that moving every point by at most  $\delta$  doesn't change the orientation of any four non-coplanar points.

Let us point out that Erickson and Kim [10] describe a construction of pairwise face-touching 3-polytopes in 3d that may provide the basis for a different representation in our model of a complete graph.

While we have shown that all graphs admit a 3d contact representation, these representations may be very non-symmetric and can have very large coordinates. This motivates the following question and specialized 3d drawing algorithms for certain classes of (non-planar) graphs; see the following subsections.

**Open Problem 1** *Is there a polynomial  $p$  such that any  $n$ -vertex graph has a 3d contact representation with convex polygons on a grid of size  $p(n)$ ?*

## 2.2 Bipartite Graphs

**Theorem 3.** *Every bipartite graph  $G = (A \cup B, E)$  admits a contact representation by convex polygons whose vertices are restricted to a cylindrical grid of size  $|A| \times 2|B|$  or to a 3d integer grid of size  $|A| \times 2|B| \times 4|B|^2$ . Such a representation can be computed in  $O(|E|)$  time.*

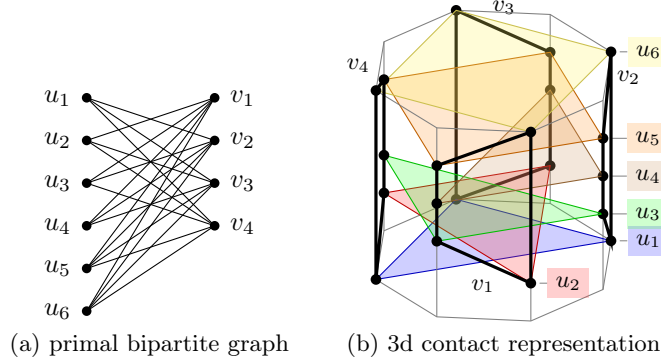


**Fig. 3:** A 3d contact representation of a bipartite graph.

*Proof.* Let  $G$  be the given bipartite graph with bipartition  $(A, B)$ . We place the vertices of the  $A$ -polygons vertically above the corners of a regular  $2|B|$ -gon in the  $xy$ -plane. Each  $A$ -polygon goes to its own horizontal plane; the planes are one unit apart. For an example, see Fig. 3. For each  $v \in B$ , the polygon  $p_v$  that represents  $v$  has a vertical edge above a unique even corner of the  $2|B|$ -gon. This vertical edge connects the bottommost  $A$ -polygon incident to  $p_v$  to the topmost  $A$ -polygon incident to  $p_v$ . All the intermediate vertices of  $p_v$  are placed on the vertical line through the clockwise next corner of the  $2|B|$ -gon. This makes sure that all vertices of  $p_v$  lie in one plane, and  $p_v$  does not intersect any other  $B$ -polygon.

Due to convexity, the interiors of the  $A$ -polygons project to the interior of the  $2|B|$ -gon. Each  $B$ -polygon projects to an edge of the  $2|B|$ -gon. Hence, the  $A$ - and  $B$ -polygons are interior-disjoint.

Note that the polygons constructed by the argument above are not *strictly convex*. We can obtain a representation with strictly convex polygons by using a finer grid  $(|A| \times |E|/2)$  on the cylinder. If we insist on representations on the integer grid, we can replace the regular  $2|B|$ -gonal base of the cylinder by a strictly convex drawing of the  $2|B|$ -cycle. Using grid points on the 2d unit parabola, we obtain a 3d representation of size  $|A| \times 2|B| \times 4|B|^2$ .  $\square$

If we apply Theorem 3 to  $K_{3,3}$ , we obtain a representation with three horizontal equilateral triangles and three vertical isosceles triangles, but with a small twist we can make all triangles equilateral. For the proof, see Appendix B.1.

**Proposition 1 (♠).** *The graph  $K_{3,3}$  admits a contact representation in 3d using unit equilateral triangles.*

### 2.3 1-Planar Cubic Graphs

A simple consequence of the circle-packing theorem [16] is that every planar graph (of minimum degree 3) is the contact graph of convex polygons in the

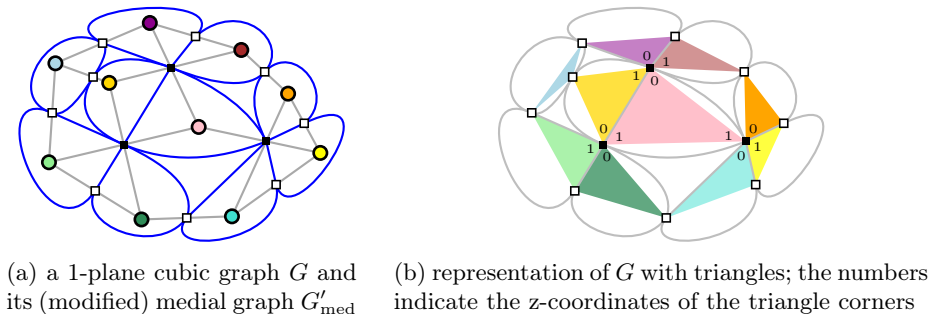


**Fig. 4:** 1-plane cubic graphs admit compact triangle contact representations.

plane. In this section, we consider a generalization of planar graphs called *1-planar graphs* that have a drawing in 2d in which every edge (Jordan curve) is crossed at most once.

Our approach to realizing these graphs will use the *medial graph*  $G_{\text{med}}$  associated with a plane graph  $G$  (or, to be more general, with any graph that has an edge ordering). The vertices of  $G_{\text{med}}$  are the edges of  $G$ , and two vertices of  $G_{\text{med}}$  are adjacent if the corresponding edges of  $G$  are incident to the same vertex of  $G$  and consecutive in the circular ordering around that vertex. The medial graph is always 4-regular. If  $G$  has no degree-1 vertices,  $G_{\text{med}}$  has no loops. If  $G$  has minimum degree 3,  $G_{\text{med}}$  is simple. Also note that  $G_{\text{med}}$  is connected if and only if  $G$  is connected.

**Theorem 4.** *Every 1-plane cubic graph with  $n$  vertices can be realized as a contact graph of triangles with vertices on a grid of size  $(3n/2-1) \times (3n/2-1) \times 3$ . Given a 1-planar embedding of the graph, it takes linear time to construct such a realization.*

*Proof.* Let  $G$  be the given 1-plane graph. Let  $G'_{\text{med}}$  be the medial graph of  $G$  with the slight modification that, for each pair  $\{e, f\}$  of crossing edges,  $G'_{\text{med}}$  has only one vertex  $v_{ef}$ , which is incident to all (up to eight) edges that immediately precede or succeed  $e$  and  $f$  in the circular order around their endpoints; see Fig. 4a. The order of the edges around  $v_{ef}$  is the obvious one. Using Schnyder's linear-time algorithm [22] for drawing 3-connected graphs<sup>5</sup> straight-line, we draw  $G'_{\text{med}}$  on a planar grid of size  $(3n/2-1) \times (3n/2-1)$ . Note that this is nearly a contact representation of  $G$  except that, in each crossing point, *all* triangles of the respective four vertices touch. Figure 4b is a sketch of the resulting drawing (without using Schnyder's algorithm) for the graph in Fig. 4a.

We add, for each crossing  $\{e, f\}$ , a copy  $v'_{ef}$  of the crossing point  $v_{ef}$  one unit above. Then we select an arbitrary one of the two edges, say  $e = uv$ . Finally we make the two triangles corresponding to  $u$  and  $v$  incident to  $v'_{ef}$  without

<sup>5</sup> If  $G'_{\text{med}}$  is not 3-connected, we add dummy edges to fully triangulate it and then remove these edges to obtain a drawing of  $G'_{\text{med}}$ .

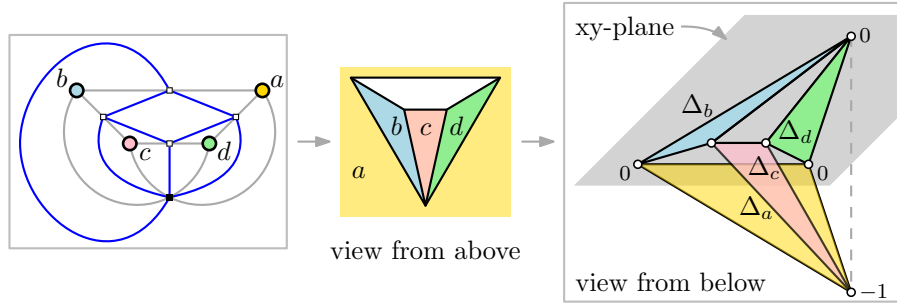


**Fig. 5:** left: graphs  $G$  (here a B-configuration, gray) and  $G'_{\text{med}}$ ; center: straight-line drawing of  $G'_{\text{med}}$ ; right: resulting 3d representation of  $G$  (numbers are  $z$ -coordinates).

modifying the coordinates of their other vertices. The labels in Fig. 4b are the resulting  $z$ -coordinates for our example; all unlabeled triangle vertices lie in the  $xy$ -plane.

If a crossing is on the outer face of  $G$ , it can happen that a vertex of  $G$  incident to the crossing becomes the outer face of  $G'_{\text{med}}$ ; see Fig. 5 where this vertex is called  $a$  and the crossing edges are  $ac$  and  $bd$ . Consider the triangle  $\Delta_a$  that represents  $a$  in  $G'_{\text{med}}$ . It covers the whole drawing of  $G'_{\text{med}}$ . To avoid intersections with triangles that participate in other crossings, we put the vertex of  $\Delta_a$  that represents the crossing to  $z = -1$ , together with the vertex of the triangle  $\Delta_c$  that represents  $c$ .

Our 3d drawing projects vertically back to the planar drawing, so all triangles are interior disjoint (with the possible exception of a triangle that represents the outer face of  $G'_{\text{med}}$ ). Triangles that share an edge in the projection are incident to the same crossing – but this means that at least one of the endpoints of the shared edge has a different  $z$ -coordinate. Hence, all triangle contacts are vertex–vertex contacts. Note that some triangles may touch each other at  $z = 1/2$  (as the two central triangles in Fig. 4b), but our contact model tolerates this.  $\square$

## 2.4 Cubic Graphs

We first solve a restricted case and then show how this helps us to solve the general case of cubic graphs.

**Lemma 2.** *Every 2-edge-connected cubic graph with  $n$  vertices can be realized as a contact graph of triangles with vertices on a grid of size  $3 \times n/2 \times n/2$ . It takes  $O(n \log^2 n)$  time to construct such a realization.*

*Proof.* By Petersen’s theorem [20], any given 2-edge-connected cubic graph  $G$  has a perfect matching. Note that removing this matching leaves a 2-regular graph, i.e., a set of vertex-disjoint cycles  $C_1, \dots, C_k$ ; see Fig. 6(a). Such a partition can be computed in  $O(n \log^2 n)$  time [9]. Let  $n = |V(G)|$  and  $n_1 = |V(C_1)|, \dots, n_k = |V(C_k)|$ . Note that  $n = n_1 + \dots + n_k$ . We now construct a planar graph  $H =$



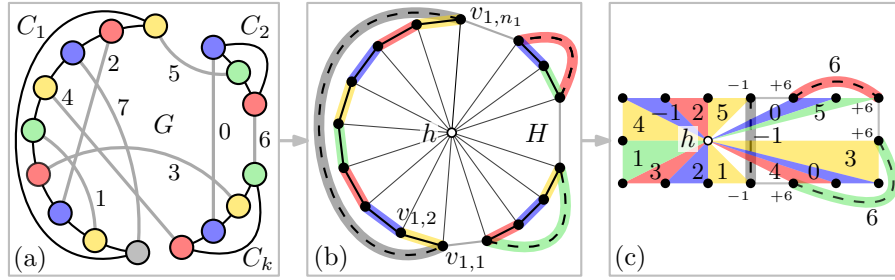


**Fig. 6:** Representing a 2-edge-connected cubic graph  $G$  by touching triangles in 3d: (a) partition of the edge set into disjoint cycles and a perfect matching (the numbers denote a permutation of the matching edges); (b) the graph  $H$ ; (c) 3d contact representation of  $G$ ; the numbers inside the triangles indicate the z-coordinates of the triangle apexes (above  $h$ ), the small numbers denote the non-zero z-coordinates of the vertices.

$(V, E)$  with  $n + 1$  vertices that will be the “floorplan” for our drawing of  $G$ . The graph  $H$  consists of an  $n$ -wheel with outer cycle  $v_{1,1}, \dots, v_{1,n_1}, \dots, v_{k,1}, \dots, v_{k,n_k}$ ,  $n$  spokes and a hub  $h$ , with additional *chords*  $v_{1,1}v_{1,n_1}, v_{2,1}v_{2,n_2}, \dots, v_{k,1}v_{k,n_k}$ . We call the edges  $v_{1,n_1}v_{2,1}, \dots, v_{k,n_k}v_{1,1}$  *dummy edges* (thin gray in Fig. 6(b) and (c)) and the other edges on the outer face the *cycle edges*.

The chords and cycle edges form triangles with apex  $h$ . More precisely, for every  $i \in \{1, \dots, k\}$ , the chord-based triangle  $\Delta v_{i,1}v_{i,n_i}h$  and the  $n_i - 1$  cycle-based triangles  $\Delta v_{i,1}v_{i,2}h, \dots, \Delta v_{i,n_i-1}v_{i,n_i}h$  together represent the  $n_i$  vertices in the cycle  $C_i$  of  $G$ . For each  $C_i$ , we still have the freedom to choose which vertex of  $G$  will be mapped to the chord-based triangle of  $H$ . This will depend on the perfect matching in  $G$ . The cycle edges will be drawn in the  $xy$ -plane (except for those incident to a chord edge); their apexes will be placed at various grid points above  $h$  such that matching triangles touch each other. The chord-based triangles will be drawn horizontally, but not in the  $xy$ -plane.

In order to determine the height of the triangle apexes, we go through the edges of the perfect matching in an arbitrary order; see the numbers in Fig. 6(a). Whenever an endpoint  $v$  of the current edge  $e$  is the *last* vertex of a cycle, we represent  $v$  by a triangle with chord base. We place the apexes of the two triangles that represent  $e$  at the lowest free grid point above  $h$ ; see the numbers in Fig. 6(c). Our placement ensures that, in every cycle (except possibly one, to be determined later), the chord-based triangle is the topmost triangle. This guarantees that the interiors of no two triangles intersect (and the triangles of adjacent vertices touch).

Now we remove the chords from  $H$ . The resulting graph is a wheel; we can simply draw the outer cycle using grid points on the boundary of a  $(3 \times n/2)$ -rectangle and the hub on any grid point in the interior. (For the smallest cubic graph,  $K_4$ , we would actually need a  $(3 \times 3)$ -rectangle, counting grid lines, in order to have a grid point in the interior, but it's not hard to see that  $K_4$  can be realized on a grid of size  $3 \times 2 \times 2$ .) If one of the  $k$  cycles encloses  $h$  in the

drawing (as  $C_1$  in Fig. 6(c)), we move its chord-based triangle from  $z = z^* > 0$  to the plane  $z = -1$ , that is, below all other triangles. Let  $i^*$  be the index of this cycle (if it exists). Note that this also moves the apex of the triangle that is matched to the chord-based triangle from  $z = z^*$  to  $z = -1$ . In order to keep the drawing compact, we move each apex with  $z$ -coordinate  $z' > z^*$  to  $z' - 1$ . Then the height of our drawing equals exactly the number of edges in the perfect matching, that is,  $n/2$ .

The correctness of our representation follows from the fact that, in the orthogonal projection onto the  $xy$ -plane, the only pairs of triangles that overlap are the pairs formed by a chord-based triangle with each of the triangles in its cycle and, if it exists, the chord-based triangle of  $C_{i^*}$  with all triangles of the other cycles. Also note that two triangles  $\Delta v_{i,j-1}v_{i,j}h$  and  $\Delta v_{i,j}v_{i,j+1}h$  (the second indices are modulo  $n_i$ ) that represent consecutive vertices in  $C_i$  (for some  $i \in \{1, \dots, k\}$  and  $j \in \{1, \dots, n_i\}$ ) touch only in a single point, namely in the image of  $v_{i,j}$ . This is due to the fact that vertices of  $G$  that are adjacent on  $C_i$  are not adjacent in the matching, and for each matched pair its two triangle apexes receive the same, unique  $z$ -coordinate.

We do not use all edges of  $H$  for our 3d contact representation of  $G$ . The spokes of the wheel are the projections of the triangle edges incident to  $h$ . The  $k$  dummy edges don't appear in the representation (but play a role in the proof of Theorem 5 ahead).  $\square$

In order to generalize Lemma 2 to any cubic graph  $G$ , we use the *bridge-block tree* of  $G$ . This tree has a vertex for each 2-edge-connected component and an edge for each bridge of  $G$ . The bridge-block tree of a graph can be computed in time linear in the size of the graph [26]. The general idea of the construction is the following. First, remove all bridges from  $G$  and, using some local replacements, transform each connected component of the obtained graph into a 2-edge-connected cubic graph. Then, use Lemma 2 to construct a representation of each of these graphs. Finally, modify the obtained representations to undo the local replacements and use the bridge-block tree structure to connect the constructed subgraphs, restoring the bridges of  $G$ . The proof is in Appendix C.

**Theorem 5 (♠).** *Every cubic graph with  $n$  vertices can be realized as a contact graph of triangles with vertices on a grid of size  $3n/2 \times 3n/2 \times n/2$ . It takes  $O(n \log^2 n)$  time to construct such a realization.*

**Corollary 2.** *Every graph with  $n$  vertices and maximum degree 3 can be realized as a contact graph of triangles, line segments, and points whose vertices lie on a grid of size  $3\lceil n/2 \rceil \times 3\lceil n/2 \rceil \times \lceil n/2 \rceil$ . It takes  $O(n \log^2 n)$  time to construct such a realization.*

*Proof.* If  $n$  is odd, add a dummy vertex to the given graph. Then add dummy edges until the graph is cubic. Apply Theorem 5. From the resulting representation, remove the triangle that corresponds to the dummy vertex, if any. Disconnect the pairs of triangles that correspond to dummy edges.  $\square$

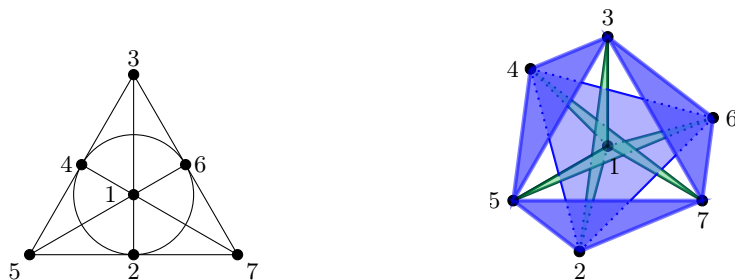


Fig. 7: The Fano plane and a 3d contact representation by touching triangles.

### 3 Hypergraphs

We start with a negative result. Hypergraphs that give rise to simplicial 2-complexes that are not embeddable in 3-space also do not have a realization using touching polygons. Carmesin's example of the cone over the complete graph  $K_5$  is such a 2-complex<sup>6</sup>, which arises from the 3-uniform hypergraph on six vertices whose edges are  $\{\{i, j, 6\} : \{i, j\} \in [5]^2\}$ . Recall that  $d$ -uniform means that all hyperedges have cardinality  $d$ . Any 3-uniform hypergraph that contains these edges also cannot be drawn. For example,  $\mathcal{K}_n^d$ , the complete  $d$ -uniform hypergraph on  $n \geq 6$  vertices for  $d = 3$  does not have a non-crossing drawing in 3d. For an elementary proof of this fact, see Theorem 9 in Appendix D.

Note that many pairs of hyperedges share two vertices in these graphs. This motivates us to consider 3-uniform *linear* hypergraphs, i.e., hypergraphs where pairs of edges intersect in at most one vertex. Very symmetric examples of such hypergraphs are *Steiner systems*. Recall that a Steiner system  $S(t, k, n)$  is an  $n$ -element set  $S$  together with a set of  $k$ -element subsets of  $S$  (called *blocks*) such that each  $t$ -element subset of  $S$  is contained in exactly one block. For examples, see Table 2. In particular, examples of 3-uniform hypergraphs are Steiner triple systems  $S(2, 3, n)$  [25]. They exist for any number  $n$  of vertices in  $\{6k + 1, 6k + 3 : k \in \mathbb{N}\}$ . Given  $n = 7, 9, 13, 15, 19, \dots$ , the corresponding 3-uniform hypergraph has  $n(n-1)/6$  hyperedges and is  $((n-1)/2)$ -regular.

First we show that the two smallest triple systems, i.e.,  $S(2, 3, 7)$  (also called the *Fano plane*) and  $S(2, 3, 9)$ , admit non-crossing drawings in 3d. See Fig. 7 for the picture of the representation of the Fano plane. The proofs of the results stated in this section can be found in Appendix E.

**Proposition 2 (♠).** *The Fano plane  $S(2, 3, 7)$  and the Steiner triple system  $S(2, 3, 9)$  admit non-crossing drawings in 3d.*

For Steiner quadruple systems  $S(3, 4, n)$ , we believe the following is true.

<sup>6</sup> Carmesin [8] credits John Pardon with the observation that the *link graph* at a vertex  $v$ , which contains a node for every edge at  $v$  and an arc connecting two such nodes if they share a face at  $v$ , must be planar for the 2-complex to be embeddable.

**Conjecture 1** *No Steiner quadruple system has a non-crossing drawing in 3d.*

We make a step towards verifying the conjecture, by showing the following.

**Observation 1** *In a non-crossing drawing of a Steiner quadruple system in 3d, every plane contains at most four vertices.*

*Proof.* Suppose that there is a drawing  $R$  and a plane  $\Pi$  that contains at least five vertices. Let  $ab$  be a maximum length edge of the convex hull of the points in the plane  $\Pi$ . No four, say  $wxyz$  in that order, can be collinear or the quadrilateral containing  $wyz$  is either  $wxyz$ , which is degenerate (a line segment), or it contains  $x$  on its perimeter but  $x$  is not a corner, a contradiction. Thus the set  $S$  of vertices on  $\Pi$  that are not on the edge  $ab$  has size at least two. If there exist  $u, v \in S$  such that  $abu$  and  $abv$  form<sup>7</sup> two distinct quadrilaterals with  $ab$  then these quadrilaterals intersect in the plane (they are both on the same side of  $ab$ ), a contradiction. If no such pair exists then  $S$  contains exactly two points and they form one quadrilateral with  $ab$ , which must contain the other vertex in  $\Pi$  (on the edge  $ab$ ) that is not a corner, a contradiction.  $\square$

Observation 1 is the starting point for the following results.

**Theorem 6 (♠).** *The Steiner quadruple system  $S(3, 4, 8)$  does not admit a non-crossing drawing in 3d.*

**Theorem 7 (♠).** *The Steiner quadruple system  $S(3, 4, 10)$  does not admit a non-crossing drawing in 3d, where all quadrilaterals representing the hyperedges are convex or all quadrilaterals are non-convex.*

## 4 Conclusion and Open Problems

We conclude the paper with two further open problems. In Section 3 we discussed the Fano plane and other Steiner systems. The Fano plane is the smallest projective plane. Can the second smallest projective plane,  $PG(3)$  (see Fig. 15 in Appendix F), which is the Steiner quadruple system  $S(2, 4, 13)$ , be drawn in 3d, such that each edge is a (convex) quadrilateral? To this end, we make the following simple observation (Observation 2 in Appendix F): Suppose that there is a drawing of  $PG(3)$  in which every edge is a convex quadrilateral, then no two quadrilaterals are coplanar. Or is it perhaps more natural to represent  $PG(3)$  by touching tetrahedra?

Our general construction in Section 2.1 implies that every  $n$ -vertex graph of maximum degree  $\Delta$  can be represented in 3d by monotone polygonal curves with at most  $\Delta - 2$  bends. Is there a natural class of graphs such that every graph  $G$  in that class can be represented by such chains with fewer than  $\Delta(G) - 2$  bends?

<sup>7</sup> In a Steiner quadruple system, every triple of vertices appears in a unique quadruple.

*Acknowledgments.* We thank Günter Rote for advice regarding strictly convex drawings of polygons on the grid. We are also grateful to the organizers of the workshop Homonolo 2017, where the project originates.

## References

1. Alam, M.J.: Contact Representations of Graphs in 2D and 3D. Ph.D. thesis, The University of Arizona (2015)
2. Alam, M.J., Evans, W., Kobourov, S.G., Pupyrev, S., Toeniskoetter, J., Ueckerdt, T.: Contact representations of graphs in 3D. In: Dehne, F., Sack, J.R., Stege, U. (eds.) Proc. Algorithms and Data Structures Symposium (WADS'15). LNCS, vol. 9214, pp. 14–27 (2015). [https://doi.org/10.1007/978-3-319-21840-3\\_2](https://doi.org/10.1007/978-3-319-21840-3_2)
3. Alam, M.J., Kaufmann, M., Kobourov, S.G.: On contact graphs with cubes and proportional boxes. In: Freivalds, R.M., Engels, G., Catania, B. (eds.) Proc. 42nd Conf. Current Trends Theory & Pract. Comput. Sci. (SOFSEM'16). LNCS, vol. 9587, pp. 107–120. Springer (2016). [https://doi.org/10.1007/978-3-662-49192-8\\_9](https://doi.org/10.1007/978-3-662-49192-8_9)
4. Brandes, U., Cornelsen, S., Pampel, B., Sallaberry, A.: Path-based supports for hypergraphs. J. Discrete Algorithms **14**, 248–261 (2012). <https://doi.org/10.1016/j.jda.2011.12.009>
5. Bremner, D., Evans, W., Frati, F., Heyer, L., Kobourov, S.G., Lenhart, W.J., Liotta, G., Rappaport, D., Whitesides, S.H.: On representing graphs by touching cuboids. In: Didimo, W., Patrignani, M. (eds.) Proc. Int. Symp. Graph Drawing (GD'12). LNCS, vol. 7704, pp. 187–198 (2012). [https://doi.org/10.1007/978-3-642-36763-2\\_17](https://doi.org/10.1007/978-3-642-36763-2_17)
6. Buchin, K., van Kreveld, M.J., Meijer, H., Speckmann, B., Verbeek, K.: On planar supports for hypergraphs. J. Graph Algorithms Appl. **15**(4), 533–549 (2011). <https://doi.org/10.7155/jgaa.00237>
7. Canny, J.F.: Some algebraic and geometric computations in PSPACE. In: Simon, J. (ed.) Proc. 20th Ann. ACM Symp. Theory Comput. (STOC'88). pp. 460–467 (1988). <https://doi.org/10.1145/62212.62257>
8. Carmesin, J.: Embedding simply connected 2-complexes in 3-space – I. A Kuratowski-type characterisation. ArXiv report (2019), <http://arxiv.org/abs/1709.04642>
9. Diks, K., Stańczyk, P.: Perfect matching for biconnected cubic graphs in  $O(n \log^2 n)$  time. In: van Leeuwen, J., Muscholl, A., Peleg, D., Pokorný, J., Rumpe, B. (eds.) Proc. 36th Conf. Current Trends Theory & Pract. Comput. Sci. (SOFSEM'10). LNCS, vol. 5901, pp. 321–333. Springer (2010). [https://doi.org/10.1007/978-3-642-11266-9\\_27](https://doi.org/10.1007/978-3-642-11266-9_27)
10. Erickson, J., Kim, S.: Arbitrarily large neighborly families of congruent symmetric convex 3-polytopes. In: Bezdek, A. (ed.) Discrete Geometry, Pure and Applied Mathematics, vol. 253, pp. 267–278. Marcel Dekker, New York (2003), in Honor of W. Kuperberg's 60th Birthday
11. Evans, W., Rzażewski, P., Saeedi, N., Shin, C.S., Wolff, A.: Representing graphs and hypergraphs by touching polygons in 3d. ArXiv report (2019), <http://arxiv.org/abs/XXXX.YYYY>
12. Felsner, S., Francis, M.C.: Contact representations of planar graphs with cubes. In: Hurtado, F., van Kreveld, M.J. (eds.) Proc. 27th Ann. Symp. Comput. Geom. (SoCG'11). pp. 315–320. ACM (2011). <https://doi.org/10.1145/1998196.1998250>

13. Gropp, H.: The drawing of configurations. In: Brandenburg, F.J. (ed.) Proc. Int. Symp. Graph Drawing (GD'95). LNCS, vol. 1027, pp. 267–276. Springer (1996). <https://doi.org/10.1007/BFb0021810>
14. Hliněný, P., Kratochvíl, J.: Representing graphs by disks and balls (a survey of recognition-complexity results). *Discrete Mathematics* **229**(1–3), 101–124 (2001). [https://doi.org/10.1016/S0012-365X\(00\)00204-1](https://doi.org/10.1016/S0012-365X(00)00204-1)
15. Johnson, D.S., Pollak, H.O.: Hypergraph planarity and the complexity of drawing Venn diagrams. *J. Graph Theory* **11**(3), 309–325 (1987). <https://doi.org/10.1002/jgt.3190110306>
16. Koebe, P.: Kontaktprobleme der konformen Abbildung. *Berichte über die Verhandlungen der Sächsischen Akad. der Wissen. zu Leipzig. Math.-Phys. Klasse* **88**, 141–164 (1936)
17. Kratochvíl, J., Matoušek, J.: Intersection graphs of segments. *J. Comb. Theory, Ser. B* **62**(2), 289–315 (1994). <https://doi.org/10.1006/jctb.1994.1071>
18. van Leeuwen, E.J., van Leeuwen, J.: Convex polygon intersection graphs. In: Brandes, U., Cornelsen, S. (eds.) Proc. 18th Int. Symp. Graph Drawing (GD'10). LNCS, vol. 6502, pp. 377–388. Springer (2011). [https://doi.org/10.1007/978-3-642-18469-7\\_35](https://doi.org/10.1007/978-3-642-18469-7_35)
19. Matoušek, J.: Intersection graphs of segments and  $\exists\mathbb{R}$ . arXiv (2014), <http://arxiv.org/abs/1406.2636>
20. Petersen, J.: Die Theorie der regulären graphs. *Acta Math.* **15**, 193–220 (1891). <https://doi.org/10.1007/BF02392606>
21. Schaefer, M.: Complexity of some geometric and topological problems. In: Eppstein, D., Gansner, E.R. (eds.) Proc. 17th Int. Symp. Graph Drawing (GD'09). LNCS, vol. 5849, pp. 334–344. Springer (2010). [https://doi.org/10.1007/978-3-642-11805-0\\_32](https://doi.org/10.1007/978-3-642-11805-0_32)
22. Schnyder, W.: Embedding planar graphs on the grid. In: Proc. 1st ACM-SIAM Symp. Discrete Algorithms (SODA'90). pp. 138–148 (1990), <https://dl.acm.org/citation.cfm?id=320176.320191>
23. Thomassen, C.: Interval representations of planar graphs. *J. Combin. Theory Ser. B* **40**(1), 9–20 (1986). [https://doi.org/10.1016/0095-8956\(86\)90061-4](https://doi.org/10.1016/0095-8956(86)90061-4)
24. Weisstein, E.W.: Steiner quadruple system. From MathWorld – A Wolfram Web Resource, <http://mathworld.wolfram.com/SteinerQuadrupleSystem.html>, accessed 2019-08-20
25. Weisstein, E.W.: Steiner triple system. From MathWorld–A Wolfram Web Resource, <http://mathworld.wolfram.com/SteinerTripleSystem.html>, accessed 2019-08-20
26. Westbrook, J., Tarjan, R.E.: Maintaining bridge-connected and bi-connected components on-line. *Algorithmica* **7**(1), 433–464 (1992). <https://doi.org/10.1007/BF01758773>
27. Zykov, A.A.: Hypergraphs. *Uspekhi Mat. Nauk* **29**(6), 89–154 (1974). <https://doi.org/10.1070/RM1974v029n06ABEH001303>

## Appendix

### A Recognizing Segments Graphs in 3d

**Theorem 1 (♠).** *Recognizing segment graphs in 3d is  $\exists\mathbb{R}$ -complete.*

*Proof.* Clearly the problem is in  $\exists\mathbb{R}$ , so let us discuss the hardness. The proof is a reduction from STRETCHABILITY, where we are given a combinatorial description of a collection of pseudolines, and we ask whether there is a collection of straight lines with the same description.

Let us start with a brief description of the original reduction, in the 2-dimensional case [19, 21]. Following Schaefer and Matoušek, we will describe the construction geometrically. This is a convenient way to describe how to obtain a graph  $G$  from the combinatorial description of the collection of pseudolines so that  $G$  is a segment intersection graph if and only if the collection of pseudolines is stretchable. More specifically, we will assume that the input combinatorial description can be arranged by straight lines, and will describe a corresponding arrangement of straight-line segments, which forms an intersection representation of the constructed graph  $G$ . Formally, the input of the recognition problem is purely combinatorial structure of the graph  $G$ , not the representation. The construction ensures that if  $G$  is a segment intersection graph, then every intersection representation by segments must be equivalent to the intended one.

The reduction starts with an arrangement of segments with the desired combinatorial description, let us call them *original segments*. We introduce three new, pairwise intersecting segments  $a$ ,  $b$ , and  $c$ , called *frame segments*. They are placed in such a way that every original segment intersects at least two frame segments, and all intersections of original segments take place inside the triangle bounded by  $a$ ,  $b$ , and  $c$ ; see Fig. 8.

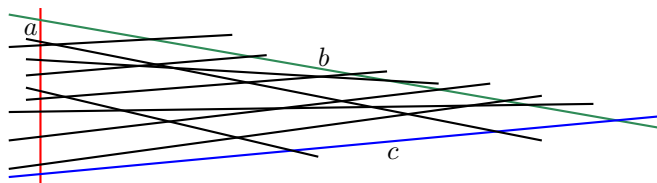


**Fig. 8:** Original segments and frame segments.

Next, for every original segment, we add many new segments, called *order segments*. Their purpose is to ensure that every representation of the constructed graph  $G$  with intersecting segments has the desired ordering of crossings of original segments; see Fig. 9 (left).

In order to show recognition hardness in 3d, we introduce some new segments (new vertices to  $G$ ), obtaining a new graph  $G'$ . For each original segment  $s$ , we

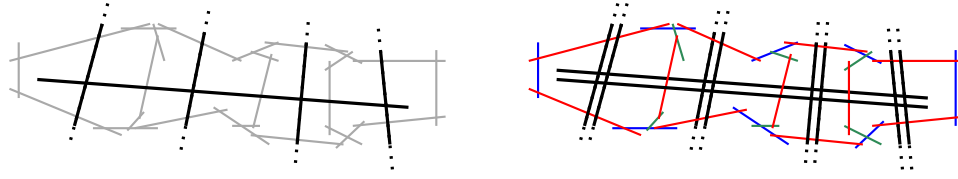


**Fig. 9:** Left: Placement of order segments (thin lines). Original segments and frame segments are drawn with thick lines. Right: Twins force all segments to be coplanar. Each segment drawn red intersects at least two original segments or twins. Each segment drawn blue intersects at least two red segments. Finally, each green segment intersects a blue and a red segment.

introduce its *twin*  $s'$ , i.e., a parallel non-overlapping segment with exactly the same neighbors as  $s$ . This completes the construction of  $G'$ .

Now let us argue that in every representation of  $G'$ , all segments from the representation are coplanar. First, note that the frame segments define a plane, let us call it the *base plane*. Moreover, recall that each original segment intersects at least two frame segments, so it also lies in the base plane. By the same argument, also twins of original segments lie in the base plane. Next, note that each order segment that intersects an original segment of  $G$  now intersects an original segment and its twin, which forces it to lie in the base plane. It is straightforward to verify that all other order segments are forced to lie in the base plane too; see Fig. 9 (right).

It is easy to verify (see, e.g., [?] for a similar argument) that  $G'$  can be represented by intersecting segments in 3d if and only if  $G'$  (and also  $G$ ) can be represented by intersecting segments in 2d if and only if the initial instance of STRETCHABILITY is a yes-instance.  $\square$

## B Contact Representations of Specific Graphs

### B.1 Representing $K_{3,3}$ with Equilateral Triangles

**Proposition 1 (♠).** *The graph  $K_{3,3}$  admits a contact representation in 3d using unit equilateral triangles.*

*Proof.* Our contact representation consists of three horizontal and three vertical unit equilateral triangles; see Fig. 10(a). The three horizontal triangles have z-coordinates 0,  $1/2$ , and 1, and are centered at the z-axis. The topmost triangle is right above the bottommost one, whereas the middle triangle is rotated by an angle  $\beta$ . In the projection on the xy-plane, all their vertices lie on a circle of radius  $\tan(30^\circ)$ ; see the small gray circle in Fig. 10(b). The figure also shows three big gray circles of radius  $\sin(60^\circ)$  (which is the height of a unit equilateral triangle) centered on the vertices of the top- and bottommost triangles. Each big circle intersects the small circle in two distinct points; in Fig. 10(b), the left one is marked with a small circle, the right one with a bigger circle. Connecting the right



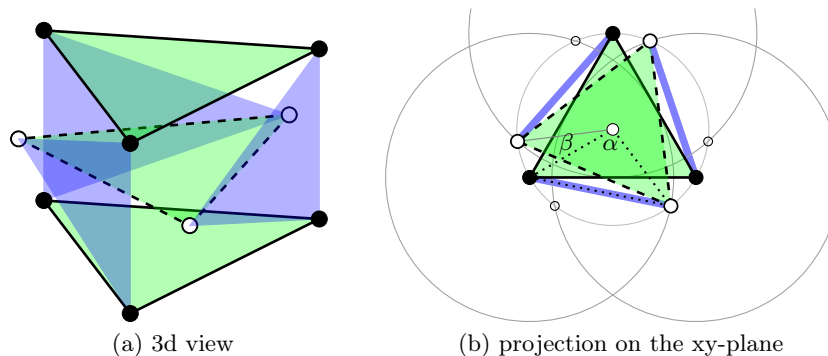


**Fig. 10:** A contact representation of  $K_{3,3}$  with unit equilateral triangles.

intersection points (bigger circles) yields the vertices of the middle horizontal triangle. The side lengths of the black dotted triangle are  $\tan(30^\circ)$ ,  $\tan(30^\circ)$ , and  $\sin(60^\circ)$ . By the law of cosines,  $\alpha = \arccos(-1/8)$ . Hence,  $\beta = 120^\circ - \alpha \approx 22.82^\circ$ .  $\square$

## B.2 Squares of Cycles

Recall that, for an undirected graph  $G$  and an integer  $k \geq 2$ , the  $k$ -th power  $G^k$  of  $G$  is the graph with the same vertex set where two vertices are adjacent when their distance in  $G$  is at most  $k$ . Note that  $C_4^2 = K_4$  is 3-regular (and can be represented by four unit equilateral triangles in the octahedron) and that, for  $n \geq 5$ ,  $C_n^2$  is 4-regular.

**Theorem 8.** *For  $n \geq 5$ ,  $C_n^2$  can be realized as the contact graph of convex quadrilaterals. In the even case, the quadrilaterals can be unit squares.*

*Proof.* For even  $n \geq 6$ ,  $C_n^2$  can be drawn as shown in Fig. 11(a), where the middle plane contains a regular  $n$ -gon and the empty faces on the top and bottom are regular  $(n/2)$ -gons. (We can get a representation with unit squares when the centers of these regular (empty) polygons are centered at the  $z$ -axis, and each vertex of the top or bottom face is on the bisecting plane of the (empty) triangular face incident to it.)

For odd  $n$ , we follow a similar approach, except the middle plane contains a regular  $(n-1)$ -gon and the top and bottom faces are  $\lceil \frac{n}{2} \rceil$ -gons. For odd  $n > 5$ , we can get a representation of  $C_n^2$  from  $C_{n-1}^2$  as shown in Fig. 11. Each vertex  $P_{i,j}$  represents the edge connecting  $i$  and  $j$ . Suppose the vertices of the regular  $(n-1)$ -gon (in the middle plane) in the representation of  $C_{n-1}^2$  are labeled  $P_{1,2}P_{2,3} \dots P_{n-2,n-1}P_{1,n-1}$  in clockwise order. (Note that this uniquely determines the labels of the other vertices.) For representing  $C_n^2$ , we re-label two of these vertices by replacing  $n-1$  with  $n$ . We then split a vertex from the top face and a vertex from the bottom face (red in Fig. 11(a)), which are on the two faces sharing the edge  $P_{n-2,n}P_{1,n}$ , into two vertices. The four new vertices

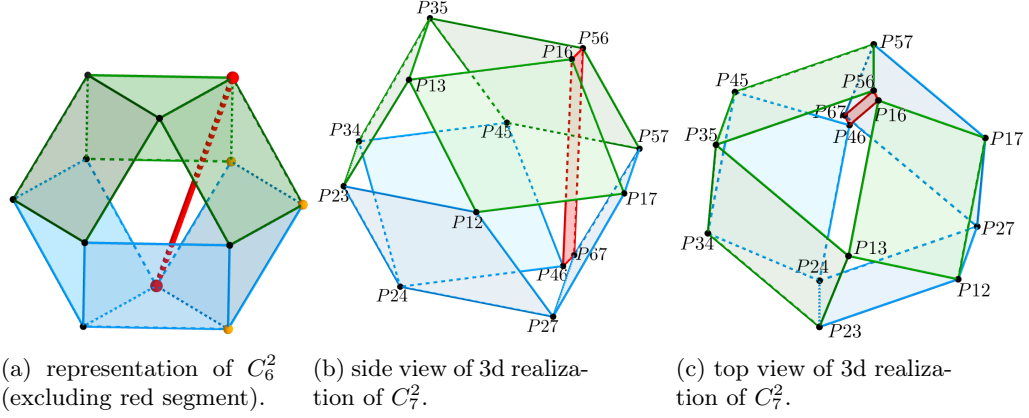


**Fig. 11:** Representation of squares of cycles. To create  $C_{2k+1}^2$  from  $C_{2k}^2$ , the two biggest vertices (red) split into two vertices and the thick (red) segment expands to a rectangle. The small vertices (black) represent the same edges as in  $C_{2k}^2$ . The bigger vertices represent new or renamed edges.

form a quadrilateral representing  $n - 1$ . (We re-label the vertices of the two faces containing the edge  $P_{n-2,n}P_{1,n}$ , but the labels of the other vertices remain unchanged.) Figures 11(b) and (c) show 3d realizations of  $C_7^2$  from different views. We can draw  $C_5^2$  (directly) using a similar structure.  $\square$

## C Representing Cubic Graphs

**Theorem 5 (♠).** *Every cubic graph with  $n$  vertices can be realized as a contact graph of triangles with vertices on a grid of size  $3n/2 \times 3n/2 \times n/2$ . It takes  $O(n \log^2 n)$  time to construct such a realization.*

*Proof.* We can assume that the given graph  $G$  is connected, otherwise we draw each connected component separately and place the drawings side-by-side. Then the bridge-block tree of  $G$  yields a partition of  $G$  into 2-edge-connected components  $G_1, \dots, G_k$ , which are connected to each other by bridges.

We go through  $G_1, \dots, G_k$  and construct floorplan graphs  $H_1, \dots, H_k$  as follows. If  $G_i$  is a single vertex, let  $H_i$  be a triangle. For an example, see  $H_6$  in Fig. 12. If a component  $G_i$  with  $n_i > 1$  doesn't contain any matching edge, that is, if all its vertices are endpoints of bridges, then let  $H_i$  be (an internally triangulated)  $n_i$ -cycle. The vertices in  $G_i$  will be represented by triangles whose bases are the edges of the cycle and whose apexes lie outside the cycle. Each apex  $v_b$  corresponds to a bridge  $b$  and will later be connected to a triangle representing the other endpoint of the bridge.

Otherwise, we remove each vertex in  $G_i$  that is incident to a bridge and connect its two neighbors, so that we can apply Petersen's theorem [20] to  $G_i$ .

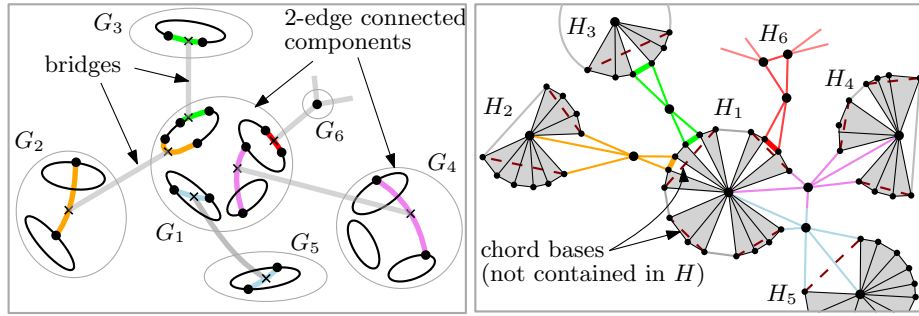


**Fig. 12:** Constructing the floorplan  $H$  of a general cubic graph

We call the new edge the *foot* of the bridge. This yields a collection of cycles and a perfect matching in  $G_i$ . As in the proof of Lemma 2,  $H_i$  is a wheel with  $|V(G_i)| + 1$  vertices, and we compute, for each component  $G_i$ , the heights of all triangle apexes. This also determines which vertices of  $G_i$  are represented by chord-based triangles. If applying Petersen's theorem to  $G_i$  gives rise to a single cycle, we consider the chord (which will be drawn at  $z = -1$ ) to simultaneously be a dummy edge (which will be "drawn" at  $z = 0$ ), so that every graph  $H_i$  has a dummy edge. (For examples, see  $H_3$  or  $H_5$  in Fig. 12.)

Let  $H$  be the disjoint union of  $H_1, \dots, H_k$ . Now we reintroduce the bridges. For every bridge  $b$ , we add a new vertex  $v_b$  to  $H$ . Each foot of  $b$  is either a cycle edge or a matching edge in some  $G_i$ , which we treat differently; see Fig. 12.

If the foot  $uw$  of  $b$  is a cycle edge, consider the two adjacent triangles in  $H_i$  that share the vertex representing the foot  $uw$ . These triangles share the hub  $h_i$  of  $H_i$  and a vertex  $v_{uw}$  on the outer face of  $H_i$ . We take the two triangles apart by duplicating  $v_{uw}$ . We connect each copy of  $v_{uw}$  to the other copy, to  $v_b$ , to  $h_i$ , and to a different neighbor along the cycle. The new edges between the two copies and between them and  $v_b$  form a triangle that represents one of the two endpoints of the bridge  $b$ ; see Fig. 13 (right).

If the foot  $uw$  of  $b$  is a matching edge, we pick a dummy edge  $xy$  on the outer face of  $H_i$ . Recall that dummy edges are the edges that connect the cycles in  $H_i$  (thin gray in Figs. 6(b) and (c)). Due to our construction,  $H_i$  contains at least one dummy edge. We remove the dummy edge  $xy$  and connect  $x$ ,  $h_i$ , and  $y$  to  $v_b$  in this order. Note that several bridge feet can be placed into the space reserved by a single dummy edge (see the bridges that connect  $H_4$  and  $H_5$  to  $H_1$  in Fig. 12 (right)).

Then we draw  $H$  in the  $xy$ -plane, using Schnyder's linear-time algorithm [22]. (In order to make  $H$  3-connected, we add edges in the outer face of  $H$  that connect the components that are leaves of the bridge-block tree.) Finally, as in the proof of Lemma 2, we insert the chord edges (at the correct heights) and extend all cycle and chord edges into triangles by placing their apexes at the locations above or below  $h_i$  that we've computed before. Whenever we place two apexes that correspond to a matching edge that is the foot of a bridge  $b$ , we use

AW: Improve correspondence between text and figure.

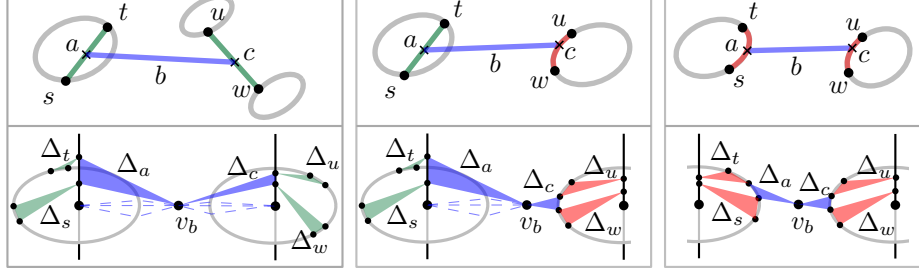


**Fig. 13:** Representation of a bridge  $b = ac$  depending on the types of its feet

two consecutive grid points, one for each apex. (If one of the apexes belongs to the chord-based triangle at  $z = -1$ , we place the other apex at  $z = 0$ .) Together with  $v_b$  (which remains on the  $xy$ -plane), the two apexes form a vertical triangle; see Fig. 13 (left). The projection of the triangle to the  $xy$ -plane is an edge of  $H$ ; the vertical (closed) slab above that edge is used exclusively by the new triangle.

To bound the grid size of the drawing, we show that  $|V(H)| \leq |E(G)|$  ( $= 3n/2$ ), by establishing an injective map from  $V(H)$  to  $E(G)$ : we map every cycle vertex in  $H$  to the ccw next cycle edge in  $H$ , which corresponds to a specific cycle edge in  $G$ . Further, we map every bridge vertex  $v_b$  to the corresponding bridge  $b$  in  $G$ . It remains to map the hubs. If a component  $H_i$  of  $H$  does not contain any matching edge (that is, all vertices in  $H_i$  are incident to bridges),  $H_i$  does not contain a hub. Otherwise, there is at least one matching edge in  $H_i$  and we map the hub  $h_i$  to that edge.

Now it is clear that the straight-line drawing of  $H$  computed by Schnyder's algorithm has size at most  $(3n/2 - 1) \times (3n/2 - 1)$ . In order to bound the height of the drawing, consider any component  $H_i$  of  $H$ . Clearly,  $H_i$  contains at most  $n/2$  matching edges. Each of these uses a grid point on the vertical line through  $h_i$ . Any matching edge can, however, be the foot of a bridge. For each bridge triangle that we insert between the apexes of two matching triangles, the height of the representation of  $H_i$  increases by one unit. On the other hand, the bridges form a matching that is independent from the matching edges. Thus, the height of  $H_i$  is at most  $n/2$ .  $\square$

## D Realizing Complete Uniform Hypergraphs by Triangles

**Theorem 9.** *For any  $n \geq 6$ ,  $\mathcal{K}_n^3$  cannot be realized by triangles in  $3d$ .*

*Proof.* Assume that a realization  $R_6$  of  $\mathcal{K}_6^3$  exists. Consider any realization  $R_5$  of  $\mathcal{K}_5^3$  that is part of  $R_6$  such that vertex  $x$  in  $\mathcal{K}_6^3 - \mathcal{K}_5^3$  is on the convex hull of  $R_6$ . Then the five vertices of  $R_5$  are either (i) in convex position or (ii) one vertex lies inside a tetrahedron that is spanned by the other four vertices. Case (i) is impossible: Let  $v$  be a vertex of  $R_5$ . Each segment from  $v$  to another vertex of

**Table 2:** The two smallest Steiner triple and quadruple systems.

$S(2, 3, 7)$	$S(2, 3, 9)$		$S(3, 4, 8)$		$S(3, 4, 10)$		
1 2 3	1 2 3	1 5 9	1 2 4 8	3 5 6 7	1 2 4 5	1 2 3 7	1 3 5 8
1 4 7	4 5 6	2 6 7	2 3 5 8	1 4 6 7	2 3 5 6	2 3 4 8	2 4 6 9
1 5 6	7 8 9	3 4 8	3 4 6 8	1 2 5 7	3 4 6 7	3 4 5 9	3 5 7 0
2 4 6	1 4 7	1 6 8	4 5 7 8	1 2 3 6	4 5 7 8	4 5 6 0	1 4 6 8
2 5 7	2 5 8	2 4 9	1 5 6 8	2 3 4 7	5 6 8 9	1 5 6 7	2 5 7 9
3 4 5	3 6 9	3 5 7	2 6 7 8	1 3 4 5	6 7 9 0	2 6 7 8	3 6 8 0
3 6 7			1 3 7 8	2 4 5 6	1 7 8 0	3 7 8 9	1 4 7 9
					1 2 8 9	4 8 9 0	2 5 8 0
					2 3 9 0	1 5 9 0	1 3 6 9
					1 3 4 0	1 2 6 0	2 4 7 0

$R_5$  lies on the convex hull of  $R_5$  so we can order these vertices as  $a, b, c$ , and  $d$  in circular order of their segments from  $v$ . But then the triangles  $vac$  and  $vbd$  intersect. In case (ii) if the tetrahedron is non-degenerate, the interior vertex  $v$  cannot be connected to  $x$ . Otherwise,  $v$  lies in (the closure of) an edge-triangle  $abc$  which intersects  $vab$ ,  $vbc$ , or  $vac$ .  $\square$

## E Representing Steiner Systems by Touching Polygons

### E.1 Steiner Triple Systems

**Proposition 2 ( $\spadesuit$ ).** *The Fano plane  $S(2, 3, 7)$  and the Steiner triple system  $S(2, 3, 9)$  admit non-crossing drawings in 3d.*

*Proof.* We first describe our construction for the Fano plane, which has seven vertices and seven hyperedges; see Table 2 and Fig. 7. We start with a unit equilateral triangle on the xy-plane centered at the z-axis representing hyperedge 642 (with vertices in ccw order). We make a copy of this triangle, lift it by one unit, and rotate it by an angle of  $\alpha$  counterclockwise around the z-axis, where  $0^\circ < \alpha < 120^\circ$  and  $\alpha \neq 60^\circ$ . (Fig. 7 uses  $\alpha = 75^\circ$ .) The copied triangle is not a hyperedge but determines the position of vertices 3, 5, and 7 (in ccw order). We place vertex 1 at  $(0, 0, 1/2)$ .

Since  $0^\circ < \alpha < 120^\circ$ , the four (blue) triangles that are not incident to 1 intersect no other triangles. Moreover, the three (green) triangles sharing vertex 1 are interior-disjoint (and non-degenerate since  $\alpha \neq 60^\circ$ ).

Now we turn to  $S(2, 3, 9)$ ; see Table 2 and Fig. 14. We start with a unit equilateral triangle on the xy-plane centered at the z-axis representing hyperedge 258 (with vertices in clockwise order). We make a copy of this triangle, lift it up by one unit, rotate it by  $60^\circ$  around the z-axis clockwise, and dilate it from its center by the factor  $1/2$ . This gives us triangle 639. We place vertices 1 and 4 at  $(0, 0, 1/2)$  and  $(0, 0, 1/4)$ , respectively. It is easy to see that the (eight) triangles induced by these (eight) vertices are all pairwise non-intersecting. Vertex 7 (not

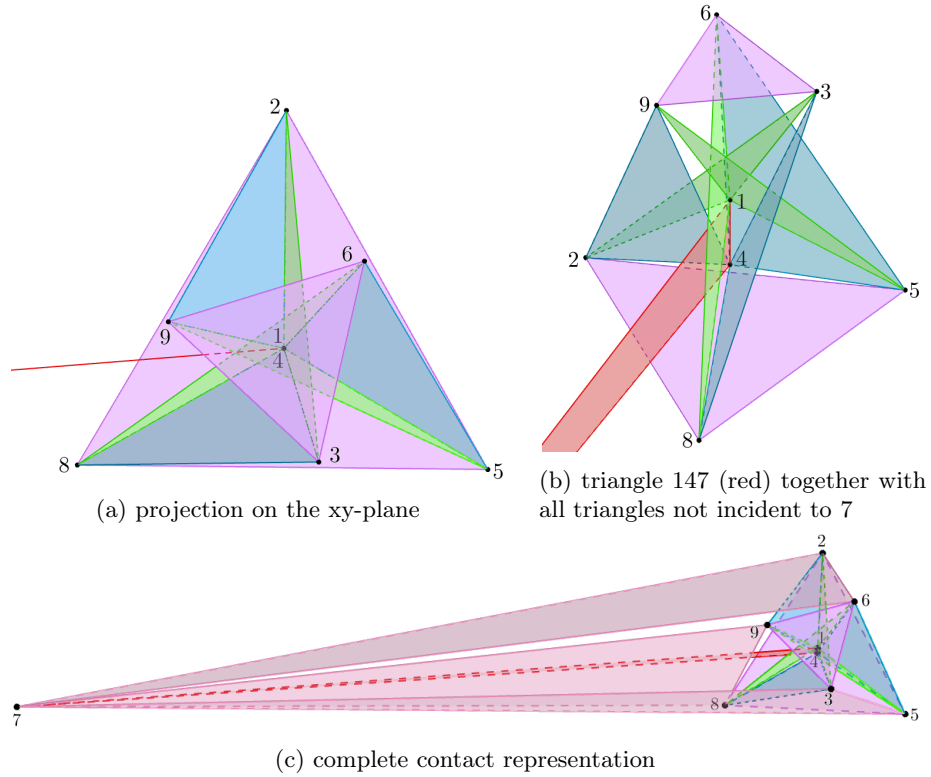


**Fig. 14:** 3d contact realization of Steiner triple system  $S(2, 3, 9)$ .

placed yet) forms triangles with segments 89, 26, 35, and 14. Note that these segments, except for 14, are on the convex hull of the vertices put so far (see Fig. 14(b)). Let  $x$  be the intersection point of the projected segments 59 and 68 after projection on the  $xy$ -plane (The projection of  $4x$  on the  $xy$ -plane lies on the red ray in Fig. 14(a).) We place 7 such that it is on the plane containing  $4x$  and perpendicular to the  $xy$ -plane; above the planes defined by 358 and 269; and below the plane defined by 168. See Fig. 14(c).  $\square$

## E.2 Steiner Quadruple Systems

**Theorem 6 (♠).** *The Steiner quadruple system  $S(3, 4, 8)$  does not admit a non-crossing drawing in 3d.*

*Proof.* The Steiner quadruple system  $S(3, 4, 8)$  has eight vertices and 14 hyperedges and is unique; see Table 2.

Assume that  $S(3, 4, 8)$  has a contact representation by quadrilaterals. Without loss of generality, assume that quadrilateral 1248 lies on the  $xy$ -plane. We

show that the supporting plane of the triple 367 is also the  $xy$ -plane, which, by Observation 1, is a contradiction.

The line through 18 and the line through 24 either intersect in a point  $v$  on the  $xy$ -plane or are parallel. The supporting planes of 1378 and 2347 both contain the line through 37 and the point  $v$  or, if  $v$  doesn't exist, the line 37 is parallel to 18 and 24. Similarly, the lines 14 and 28 intersect in a point  $w$  on the  $xy$ -plane or are parallel. The supporting planes of 1467 and 2678 both contain the line through 67 and the point  $w$  or, if  $w$  doesn't exist, the line 67 is parallel to 14 and 28. Again, a similar statement holds for the intersection  $u$  on the  $xy$ -plane of the lines 12 and 48. The supporting planes of 1236 and 3468 both contain the line 36 and the point  $u$  or, if  $u$  doesn't exist, the line 36 is parallel to 12 and 48. These conditions imply that the supporting plane of 367 is parallel to the  $xy$ -plane. Since at least one of  $u$ ,  $v$ , and  $w$  exists and is in the  $xy$ -plane, 367 lies in the  $xy$ -plane, contradicting Observation 1.  $\square$

To prove Theorem 7, we will need an auxiliary lemma.

**Lemma 3.** *Let  $H$  be a hypergraph whose edge set contains the subset  $F = \{abcd, abuv, cduv, acwx, bdwx, adyz, bcyz\}$ . Then  $H$  does not admit a contact representation by quadrilaterals in which the edges in  $F$  are all convex or all non-convex.*

*Proof.* Suppose that  $H$  has a representation where the hyperedges in  $F$  are all convex. Let  $e = abcd$ . (Note that we identify  $e$  with the quadrilateral that represents it.) No matter which segments form the diagonals of  $e$  ( $ab$  and  $cd$ ,  $ac$  and  $bd$ , or  $ad$  and  $bc$ ), there is a pair ( $uv$ ,  $wx$ , or  $yz$ ) that forms two hyperedges with the two diagonals. We assume that the diagonals are  $ab$  and  $cd$  forming hyperedges  $abuv$  and  $cduv$ . Due to the convexity of the quadrilateral  $e$ ,  $ab$  and  $cd$  intersect. Hence, since  $abuv$  and  $cduv$  are convex, one of the hyperedges  $abuv$  and  $cduv$  must be drawn above  $e$ , and one below  $e$ . This yields the desired contradiction since  $u$  and  $v$  are contained in both of these hyperedges.

Suppose that  $H$  has a representation where the hyperedges in  $F$  are all non-convex. We may assume that the diagonals of  $e$  are again  $ab$  and  $cd$ , that  $ab$  is not contained in  $e$ , and that  $c$  lies on the convex hull of  $e$  whereas  $d$  does not. Let  $x$  be the intersection point of the supporting lines of  $ab$  and  $cd$ . Note that  $x$  lies on  $ab$ . This is due to the fact that  $cd$  is incident to  $c$  and lies inside the angle  $\angle acb$ . The supporting planes of the quadrilaterals  $abuv$  and  $cduv$  intersect in a line  $\ell$  that intersects the supporting plane of  $e$  in  $x$ . Clearly,  $u$  and  $v$  must lie on  $\ell$  since they are part of both quadrilaterals  $abuv$  and  $cduv$ .

We consider two cases. In the first case,  $u$  and  $v$  lie on different halflines of  $\ell$  with respect to  $x$ . Then vertices  $a$ ,  $b$ ,  $u$ , and  $v$  are in convex position, forming a convex quadrilateral with diagonals  $uv$  and  $ab$ . Note that it is not possible to connect points in convex position with straight-line segments to form a non-degenerate non-convex polygon. This contradicts the fact that all quadrilaterals in  $F$  must be non-convex. In the second case,  $u$  and  $v$  lie on the same halfline of  $\ell$  with respect to  $x$ . But then vertices  $c$ ,  $d$ ,  $u$ , and  $v$  are in convex position

since also  $c$  and  $d$  lie on the same halfline with respect to  $x$ . This again yields the desired contradiction.  $\square$

Now we are ready to prove the following.

**Theorem 7 ( $\spadesuit$ ).** *The Steiner quadruple system  $S(3, 4, 10)$  does not admit a non-crossing drawing in 3d, where all quadrilaterals representing the hyperedges are convex or all quadrilaterals are non-convex.*

*Proof.* The Steiner quadruple system  $S(3, 4, 10)$  has ten vertices and 30 hyperedges and is unique; see Table 2. Note that  $S(3, 4, 10)$  satisfies the assumptions of Lemma 3 for  $a = 1, b = 4, c = 2, d = 5, u = 7, v = 9, w = 6, x = 0, y = 3$ , and  $z = 8$ , i.e., it contains the set of edges  $F = \{1245, 1260, 4560, 1479, 2579, 1538, 2438\}$ . The claim follows from Lemma 3.  $\square$

## F Discussion about Projective Planes

Note that in Steiner quadruple systems many pairs of edges intersect in two vertices. In a projective plane, every pair of edges (called *lines*) intersects in exactly one vertex (*point*). So maybe this is easier? Recall that any projective plane fulfills the following axioms:

- (P1) Given any two distinct points, there is exactly one line incident to both of them.
- (P2) Given any two distinct lines, there is exactly one point incident to both of them.
- (P3) There are four points such that no line is incident to more than two of them. (Non-degeneracy axiom)

Every projective plane has the same number of lines as it has points. The projective plane of order  $N$ ,  $PG(N)$ , has  $N^2 + N + 1$  lines and points and there are  $N + 1$  points on each line, and  $N + 1$  lines go through each point. Equivalently, we can see  $PG(N)$  as a Steiner system.  $S(2, N + 1, N^2 + N + 1)$ .

Note, however, that any contact representation of  $PG(3)$  by convex quadrilaterals contains a contact representation of  $S(2, 3, 9)$  by triangles: just drop one of the 13 quadruples of  $PG(3)$  and remove its four vertices from all quadruples. This yields twelve triples with the property that any pair of vertices is contained in a unique triple (P1).

**Observation 2** *Suppose that there is a realization of  $PG(3)$  with convex quadrilaterals, then no two quadrilaterals are coplanar in such a realization.*

*Proof.* For the sake of contradiction, suppose that two quadrilaterals,  $q_1$  and  $q_2$ , lie in the same plane  $\Pi$  in a realization  $R$  of  $PG(3)$  with convex quadrilaterals. Every two quadrilaterals share exactly one vertex (P2), hence, we can write  $q_1$  and  $q_2$  as  $q_1 = u_1u_2u_3w$  and  $q_2 = v_1v_2v_3w$ . Since every pair of vertices appears in exactly one quadrilateral (P1), each pair  $u_iv_j$  with  $i, j \in \{1, 2, 3\}$  is contained in



A	B	C	D
A	1	2	3
A	4	5	6
A	7	8	9
B	1	4	7
B	2	5	8
B	3	6	9
C	1	5	9
C	2	6	7
C	3	4	8
D	1	6	8
D	2	4	9
D	3	5	7

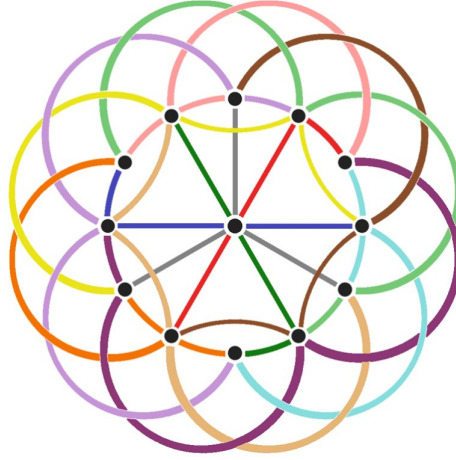


**Fig. 15:** The second smallest discrete projective plane  $PG(3)$ , which is a 4-regular 4-uniform hypergraph with 13 vertices and 13 hyperedges. The drawing is taken from <https://puzzlewocky.com/games/the-math-of-spot-it/>.

a different quadrilateral. Since the quadrilaterals in  $R$  are convex, each line segment  $\overline{u_i v_j}$  is contained in the unique quadrilateral containing vertices  $u_i$  and  $v_j$ . Since  $u_i$  and  $v_j$  lie in  $\Pi$ ,  $\overline{u_i v_j}$  also lies in  $\Pi$ . As a result,  $\Pi$  contains a planar (straight-line) drawing of  $K_{3,3}$  (with vertex set  $\{u_1, u_2, u_3\} \cup \{v_1, v_2, v_3\}$ ), which yields the desired contradiction.  $\square$